

The Influence of Harmonic Content on the RMS Value of Electromagnetic Fields Emitted by Overhead Power Lines

Jozef Bendík ^{*,†} , Matej Cenký [†]  and Žaneta Eleschová [†] 

Faculty of Electrical Engineering and Information Technology, Slovak University of Technology in Bratislava, Ilkovičova 3, 81 219 Bratislava, Slovakia; matej.cenky@stuba.sk (M.C.); zaneta.eleschova@stuba.sk (Ž.E.)

* Correspondence: jozef.bendik@stuba.sk

[†] These authors contributed equally to this work.

Abstract: This paper investigates the influence of harmonic content on the root mean square value of electromagnetic fields emitted by overhead power lines. The paper presents a methodology to assess the intensity of electric field and magnetic flux density, incorporating both fundamental frequencies and harmonics. The results of our calculations indicate that harmonic distortion in current waveforms can significantly increase the RMS value of magnetic flux density but its effect on electric field intensity is minimal. Additionally, our findings highlight a potential increase in induced voltages on buried or overhead steel pipelines in the vicinity of OPLs, which could pose risks such as pipeline damage and increased corrosion. This underscores the importance of considering harmonic content in EMF exposure evaluations to address both health risks and potential infrastructure impacts comprehensively. Effective harmonic management and rigorous infrastructure monitoring are essential to prevent potential hazards and ensure the reliability of protective systems.

Keywords: harmonics; magnetic flux density; intensity of electric field; overhead power lines; root mean square; health



Citation: Bendík, J.; Cenký, M.; Eleschová, Ž. The Influence of Harmonic Content on the RMS Value of Electromagnetic Fields Emitted by Overhead Power Lines. *Modelling* **2024**, *5*, 1519–1531. <https://doi.org/10.3390/modelling5040079>

Academic Editor: Reza Abedi

Received: 22 August 2024

Revised: 2 October 2024

Accepted: 11 October 2024

Published: 16 October 2024



Copyright: © 2024 by the authors. Licensee MDPI, Basel, Switzerland. This article is an open access article distributed under the terms and conditions of the Creative Commons Attribution (CC BY) license (<https://creativecommons.org/licenses/by/4.0/>).

1. Introduction

Overhead power lines (OPL) produce electromagnetic fields (EMF) at low frequencies. These EMFs have a typical power frequency of 50 Hz or 60 Hz [1] and are classified as extremely low-frequency fields (ELFs). In general, ELF are categorized as a field within the range of 0 Hz to 300 Hz [2]. There are two main reasons why it is necessary to quantify ELF from OPL:

- Possible health effects on the human body and potential interference of these fields with medical devices.
- Technical aspects of the issue. ELF causes inductive and capacitive coupling between objects, which ultimately results in induced voltages and currents in the surrounding infrastructure, such as pipeline networks and metallic telecommunication lines. These voltages and currents pose a potential danger upon contact for workers or the public [3].

The potential health risks associated with exposure to Extremely Low Frequency (ELF) fields from OPL have generated debate. While ELF is classified as non-ionizing radiation and generally deemed safe by regulatory bodies, some studies suggest a possible link to childhood leukemia, though the evidence remains inconclusive and disputed [4]. Research into ELF association with other cancers, such as brain tumors and breast cancer, has also produced mixed results [5,6].

Despite uncertainties, regulatory bodies like the International Commission on Non-Ionizing Radiation Protection (ICNIRP) have set exposure guidelines to minimize the potential risks [7]. A notable concern is the interference of ELF fields with Active Implanted Medical Devices (AIMD). The European Union's Directive 2013/35/EU and its 2015 guide

highlight that electric fields greater than 5 kV/m, common under Extra High Voltage (EHV) lines with low ground clearance, may pose risks to workers with AIMD [8–11].

Several countries and organizations have created their own exposure limits and reference values for the public and workers. These reference levels of exposure to ELF can vary according to international standards. An extensive comparison of international policies on electromagnetic fields including power frequency and radio frequency fields can be found in [12]. The reference levels for the Slovak republic are shown in Table 1 [13].

Concerns over health risks have prompted the establishment of new design standards for power lines. Electromagnetic field effects are now a critical factor in the construction of transmission lines [14]. As operational safety around OPL gains importance, more comprehensive project planning is required.

As shown in Table 1 and illustrated in the graphs in Figures 1 and 2, the exposure limits vary across different frequencies. The included graphs and tables show the dependence of the limits on frequency only for low frequencies, for which the possible values of higher harmonics are clearly defined by the qualitative standard EN 50160:2022 [15] and IEEE Std 519-2014 [16]. It is suggested that these exposure limits are designed to shield individuals from the energy levels present within the field. Nevertheless, many situations occur where the field is not produced by a perfect sine wave. In fact, the predominance of fields is characterized by a lack of pure sinusoidal nature. The foundational exposure limit individually assesses the frequencies through their root mean square value (RMS).

Table 1. Reference levels in Slovak republic for exposure to time-varying electric and magnetic fields (unperturbed RMS values) for distinct frequencies.

Frequency Hz	Intensity of Electric Field E_{rms} [kV·m ⁻¹]	Magnetic Flux Density B_{rms} [μ T]
50	5.000	100.0
150	1.666	33.33
250	1.000	20.00
550	0.454	9.090
1000	0.250	6.250
3000	0.087	6.250

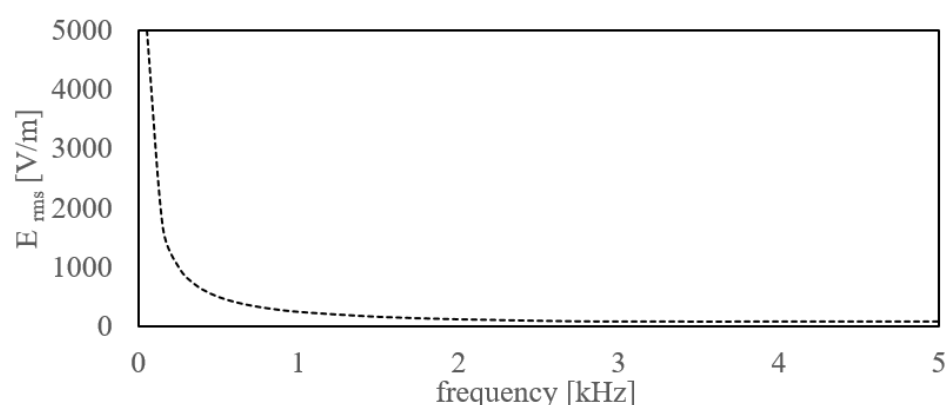


Figure 1. Graph showing the dependency of exposure limit E_{rms} from frequency.

The limitations on OPL ELF values were established primarily to protect health. However, it is the technical aspects, particularly the hazardous and disruptive effects such as induced voltages on conductive objects and discharge currents passing through a person in case of contact with such an object that pose the greater risk. Depending on whether an object near an OPL is subject to capacitive, inductive coupling, or a combination of both, various issues can arise. Additionally, the problems differ based on whether the line is experiencing a fault condition or is in steady-state operation:

- Fault conditions of OPL: Individuals in direct contact with pipes that have induced voltages are at risk. The standard EN 50443 defines the maximum allowable induced voltages depending on the duration of the fault [17].
- Steady-state operation of OPL: Although these induced and current voltages are typically low, their persistent nature can cause misfunctions in cathodic protection systems for pipelines. Standard EN 50443 sets a limit of 60 V, while Standard EN ISO 18086 adjusts this value to 15 V for proper operation of protection systems [18]. In practice, the ratio of induced voltage to the pipe to e potential, E_{on} , must be considered. E_{on} is the potential measured while the cathodic protection system is operating. Safe values in such scenarios are typically in the range of a few volts, and even slight increases over time can significantly reduce pipeline lifespan.

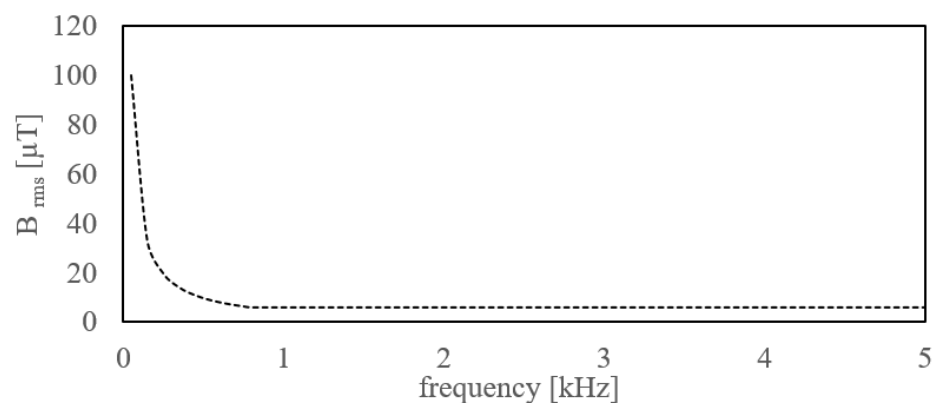


Figure 2. Graph showing the dependency of exposure limit B_{rms} from frequency.

In general, many articles and studies have greatly covered the topic of ELF emitted by OPL lines in recent decades. The comparison and methodology for the calculation of electric field intensity and magnetic flux induction for typical HV and EHV OPL configuration can be found in [11,19–23]. Approaches for optimization using advanced genetic and particle swarm algorithms are shown in [24]. The basic theory for calculation is well described in [25] and CIGRE brochures. The research comparing the ELF generated by a 110 kV double-circuit OPL through measurements and numerical simulations is presented in [26]. However, the impact of harmonics content in currents and voltages on the values of ELF is presented in very few of the studies. A paper by Mujezinović et al. from 2022 highlights the significance of accurately determining the contributions of individual harmonic components to the total magnetic flux density, showcasing the practical application of the proposed calculation method in analyzing overhead line configurations. Their results show that magnetic flux density can increase by 5% for 110 kV lines by including harmonics in the calculation [27]. The effects of VSC-HVDC harmonics from converter stations on OPL are analyzed in [28]. The influence of harmonics in current on the magnetic flux density for a double circuit EHV line is analyzed in [29]. Their results show that harmonics can increase the RMS value of the field in order of percent up to 4%, depending on the THD (total harmonic distortion) of current. Another approach to the problem of harmonics is presented in a paper from 2019, which presents a model for analyzing power line harmonic radiation in the ionosphere [30].

The aim of this article is to analyze potential increases in ELF values due to higher harmonics in voltage and current during the steady-state operation of OPL. Our study examines the maximum possible increases in the RMS values of magnetic field induction and electric field intensity around 110 kV lines. This maximum increase is directly attributed to the consideration of higher harmonic limits as defined by EN 50160:2022 for HV OPL [15], and IEEE Std 519-2014 for current distortion [16].

Novelty of the Work

This paper presents a novel approach by consolidating and synthesizing methodologies for assessing ELF fields from OPL, which are typically fragmented across various studies and standards. It introduces a unique method for calculating the maximum RMS values of E and B fields, considering the maximum harmonic distortion caused by voltage and current, strictly adhering to standards such as EN 50160:2022 and IEEE Std 519-2014. Additionally, the paper discusses the potential consequences of ELF fields on human health and surrounding infrastructure, providing a holistic view that is crucial for developing effective safety guidelines and design standards. This comprehensive and precise approach represents a significant advancement in the field, addressing both health risks and technical impacts.

The following paper is organized as follows. Section 2 describes the basic methodology for EMF from OPL evaluation. Section 3 details the ELF calculation produced by the specific 110 kV OPL. Section 4 analyses the results and compares the field's total RMS values with base power frequency field values. Section 5 discusses the current THD values magnetic flux density increase over base frequency.

2. Materials and Methods

In the following part, the basic terminology used for the evaluation of EMF for different frequencies is described. All fields analyzed in this paper are referred to as quasi-static. Time-varying EMF is considered quasi-static when the temporal changes in EMF propagation can be considered negligible at finite speeds [31,32].

2.1. Terminology

Marking used in the following text:

- \vec{E} vector is represented by an arrow
- \hat{E} phasor is represented by a hat over the character
- E_{rms} root mean square value of the quantity
- E_m magnitude of quantity
- E_{m_x} magnitude of a quantity in a specific x direction
- $E_{i_x}(t)$ time-dependent value of a given quantity in the x direction,

The quasi-stationary nature of the field stems from its low frequency, allowing for the separate calculation of each component of ELF. This simplifies calculations, utilizing basic electrostatics to compute the intensity of the electric field and magnetostatics to determine the magnetic flux density. The voltage and current sources of these fields are represented in phasor form [25].

The following relations represent the mathematical description of magnetic flux density and intensity of electric field for a single frequency in an n-conductor system. These relations are valid only in the case of a quasi-stationary field. The extension of this description to higher harmonics is provided in Section 2.5. The superposition of \vec{E} and \vec{B} involves adding the fields generated by individual charges Q and currents I , Equations (1) and (2) [31,32].

$$\vec{E} = \vec{E}_1(Q_1) + \vec{E}_2(Q_2) + \dots + \vec{E}_n(Q_n) \quad (1)$$

$$\vec{B} = \vec{B}_1(I_1) + \vec{B}_2(I_2) + \dots + \vec{B}_n(I_n) \quad (2)$$

The EMF field near the OPL is described in this paper using phasors and vectors. A vector is characterized by a magnitude and an angle in space or by three spatial components, Equation (3) [1].

$$\vec{E} = [E_x; E_y; E_z] \quad (3)$$

Phasor is a quantity with a sinusoidal time variation described by a magnitude and a phase angle, Equation (4). Angle ϕ_x describes phase shift [1].

$$E_{i_x}(t) = E_{m_x} \cos(\omega t + \phi_x) \Rightarrow \hat{E}_{m_x} = E_{m_x} \angle \phi_x \quad (4)$$

The root mean square representation is as follows:

$$\hat{E}_{rms_x} = \frac{E_{m_x}}{\sqrt{2}} \angle \phi_x \quad (5)$$

Three perpendicular vector components can be phasors, each having different magnitudes and phase angles. These components are referred to as the phasor-vector, Equation (6) [33].

$$\hat{\vec{E}}_{rms} = [\hat{E}_{rms_x}; \hat{E}_{rms_y}; \hat{E}_{rms_z}] = [E_{rms_x} \angle \phi_x; E_{rms_y} \angle \phi_y; E_{rms_z} \angle \phi_z] \quad (6)$$

The same equation follows for magnetic flux density B .

The predominant approach for characterizing the harmonic field is through scalar quantity. The scalar RMS value of the field can be derived from the phasor-vector definition as follows:

$$E_{rms} = \sqrt{\Re\{\hat{\vec{E}}_{rms}\}^2 + \Im\{\hat{\vec{E}}_{rms}\}^2} \quad (7)$$

$$E_{rms} = \sqrt{\Re\left[\sqrt{\hat{E}_{rms_x}^2 + \hat{E}_{rms_y}^2 + \hat{E}_{rms_z}^2}\right]^2 + \Im\left[\sqrt{\hat{E}_{rms_x}^2 + \hat{E}_{rms_y}^2 + \hat{E}_{rms_z}^2}\right]^2} \quad (8)$$

2.2. Position of Calculation

In determining EMF, various methods and locations can be considered. For the sake of simplicity in this paper, the field is computed along the horizontal axis perpendicular to the axis of a symmetrical span Figure 3, positioned at a height of 1.8 m above flat terrain. The conductors are assumed to be infinitely long and positioned at the lowest point of their actual sag.

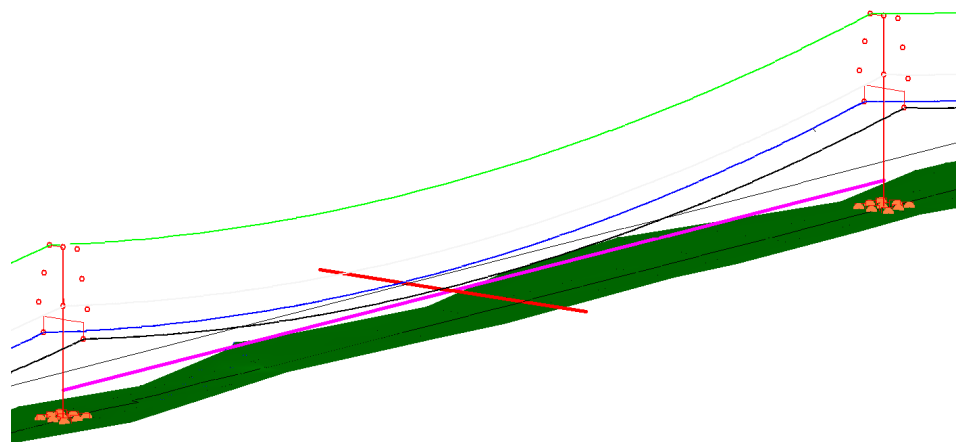


Figure 3. Illustration of position of EMF calculation, red line perpendicular to span axis.

Consider point P as the observation point where we intend to evaluate the electric field intensity. Vector \vec{r}_p points from the origin to P. Vector \vec{r}_o points from the origin to conductor element. The vector \vec{r} originates from an element of the conductor dl and extends toward the observer P. The positions of the vectors in relation to P are shown in Figure 4.

\vec{r} can be expressed as follows:

$$\vec{r} = (\vec{r}_p - \vec{r}_o) \quad (9)$$

where \vec{r}_p denotes the vector from the origin of the coordinate system to observer P, and \vec{r}_o indicates the vector from the origin of the coordinate system to the element of conductor dl .

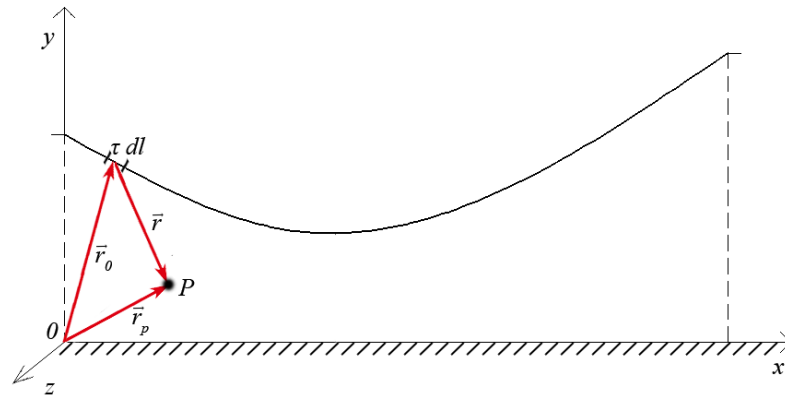


Figure 4. The positions of the vectors \vec{r} , \vec{r}_0 , \vec{r}_p around catenary curve in relation to the observer P.

2.3. Intensity of Electric Field

The calculation of E is based on Coulomb's law. The analytical expression of Coulomb's law, after substituting Equation (9), is as follows:

$$\vec{E} = \int_l d\vec{E} = \frac{1}{4\pi\epsilon_0} \int_l \frac{\tau dl}{|\vec{r}_p - \vec{r}_0|^3} (\vec{r}_p - \vec{r}_0) \quad (10)$$

where τ is the linear charge density and ϵ_0 the permittivity of the free space. In a 2D space where the conductors' cross-section lies in a plane, this solution can be simplified to the following:

$$\vec{E} = \frac{1}{4\pi\epsilon_0} \frac{\tau}{|\vec{r}_p - \vec{r}_0|^3} (\vec{r}_p - \vec{r}_0) \quad (11)$$

The electric field arises from charges in both the conductors and the terrain with a boundary potential $\varphi = 0$. The distribution and density of charges on this plate are uneven. This problem is solved using the method of image charges.

The intensity of the electric field \vec{E} at the observer point P is the sum of electric intensities created by each conductor k , including both real and mirrored conductors (subscript with apostrophe).

$$\vec{E} = \vec{E}_1 + \dots + \vec{E}_k + \vec{E}_{1'} + \dots + \vec{E}_{k'} \quad (12)$$

Linear charge density can be calculated from known line-to-ground voltages and the geometry of the system. For an infinite straight conductor, the linear charge density can be calculated by Equation (13), where $[\tau_k]$ is the vector of linear charge densities in the conductors k , $[P]$ is a 2D matrix of the maxwell potential coefficients, $[U_k]$ is the vector of voltages. The diagonal components $[P] P_{kk}$ are the self-potential coefficient of the conductor k and the non-diagonal components P_{kj} are the mutual potential coefficients of the conductors k and j .

$$[\tau_k] = [P]^{-1}[U_k] \quad (13)$$

The components of the $[P_{kk}]$ are computed as follows

$$P_{kk} = \frac{1}{2\pi\epsilon_0} \ln\left(\frac{2h_k}{R_k}\right) \quad (14)$$

$$P_{kj} = \frac{1}{2\pi\epsilon_0} \ln\left(\frac{D'_{kj}}{D_{kj}}\right) \quad (15)$$

where h_k is the height of the conductor element k above ground, R_k is the radius of the conductor k , D_{kj} is the distance between the elements of the conductors k and j , D'_{kj} is the distance between the element of the conductor k and the mirror element of the conductor j .

When computing the harmonically oscillating field with the intensity \hat{E} represented as a phasor-vector, we utilize the RMS phasor of the line-to-ground voltage of each conductor \hat{U}_{rms_k} as input. Equation (13) can be rewritten as follows:

$$[\hat{r}_{rms_k}] = [P_{kk}]^{-1}[\hat{U}_{rms_k}] \quad (16)$$

The intensity of the electric field under the OPL consisting of k conductors is then calculated:

$$\hat{E}_{rms} = \sum_{k=1}^k \left[\hat{E}_{rms_k} + \hat{E}_{rms_k'} \right] \quad (17)$$

2.4. Magnetic Flux Density

The computation of magnetic flux density relies on the Biot–Savart law [34,35] where $d\vec{l}$ represents the vector element of the conductor. The path integral is determined along the path of the conductor. Here, μ_0 denotes the permeability of free space, while I represents the current flowing through the conductor.

$$\vec{B} = \frac{\mu_0}{4\pi} \int_a \frac{Id\vec{l} \times (\vec{r}_p - \vec{r}_0)}{|\vec{r}_p - \vec{r}_0|^3} \quad (18)$$

By simplifying the computation for an infinitely straight conductor in a 2D plane, we obtain the following equation, where \vec{l} represents a unit vector perpendicular to our 2D plane.

$$\vec{B} = \frac{\mu_0}{4\pi} \frac{I\vec{l} \times (\vec{r}_p - \vec{r}_0)}{|\vec{r}_p - \vec{r}_0|^3} \quad (19)$$

When magnetic flux density is generated by multiple conductors, the outcome is the superposition of fields at every point observed from each conductor k . Similar to the case of the intensity of electric fields, we represent the current in the form of the phasor, and we obtain the following:

$$\hat{B}_{rms} = \sum_{k=1}^k [\hat{B}_{rms_k}] = \sum_{k=1}^k \left[\frac{\mu_0}{4\pi} \frac{\hat{I}_{rms_k} \vec{l} \times (\vec{r}_p - \vec{r}_{0k})}{|\vec{r}_p - \vec{r}_{0k}|^3} \right] \quad (20)$$

2.5. Root Mean Square of Waveform

Let us assume that the harmonic content of the waveform is known. We will use the current waveform for the explanation consisting of the frequencies of n harmonics.

$$I(\omega t) = I_1(\omega t) + I_2(2\omega t) + \dots + I_n(n\omega t) \quad (21)$$

The total RMS value of the given waveform is as follows:

$$I_{rms} = \sqrt{I_{1rms}^2 + I_{2rms}^2 + \dots + I_{nrms}^2} \quad (22)$$

The same principle can be applied to each individual component of the phasor-vector, as well as to voltages in a similar manner.

3. Calculation

A calculation of the total RMS value of magnetic flux density and intensity of the electric field has been performed to demonstrate the influence of harmonics in the current and voltage

waveform. The EMF was calculated for a 110 kV double system (2×110 SUDOK, vertical phase system configuration), which is a typical HV OPL. The parameters of the system are listed in Table 2, and the geometry and phase configuration are detailed in Table 3. These parameters represent the typical 110 kV line in the Slovak Republic [11]. The chosen phase configuration, with the same phase in each arm, maximizes the overall value of the EMF components. The calculation was conducted at the center of the line, with the ground clearance of the lower conductors set to be 6 m. Additionally, the calculation was performed on a line perpendicular to the axis of the line at the height of 1.8 m above the flat ground.

The stated current values (700 A in this case) are not commonly achieved in practice and depend on the current load of the line, which changes dynamically over time. Nevertheless, legislation requires the calculation of EMF for the worst-case scenario of conductor loading and at the lowest possible height of the bottom conductor above the ground for which the OPL is designed.

Table 2. Calculation parameters.

Type of tower	SUDOK
No. of systems	2
No. of ground wires	1
Phase to phase voltage	121 kV
Current per phase	700 A
Type of phase conductor	ACSR 445/74
Type of phase conductor	ACSR 180/59
Ground clearance	6 m

Table 3. Geometry of the tower and phase configuration.

Configuration		Position of Conductors on Tower	
		Height [m]	Displacement [m]
System 1	Phase 1	16.2	−3
	Phase 2	20.0	−3.8
	Phase 3	23.8	−3
System 2	Phase 1	16.2	3
	Phase 2	20.0	3.8
	Phase 3	23.8	3
Ground wire		27.4	0

Harmonic distortion up to the 40th harmonic was analyzed, as shown in Figure 5. The harmonic spectrum of the voltage represents the maximum allowable harmonic distortion as defined by EN 50160:2022 for HV OPL [15], with a calculated total harmonic distortion (THD) of 8.1%. EN 50160:2022 does not specify THD or harmonic spectrum for current. Therefore, the harmonic spectrum of the current represents the maximum allowable harmonic distortion defined by IEEE Std 519-2014 for HV OPLs with a maximum demand current of over 1000 A [16]. The calculated THD of the current is 37.1%.

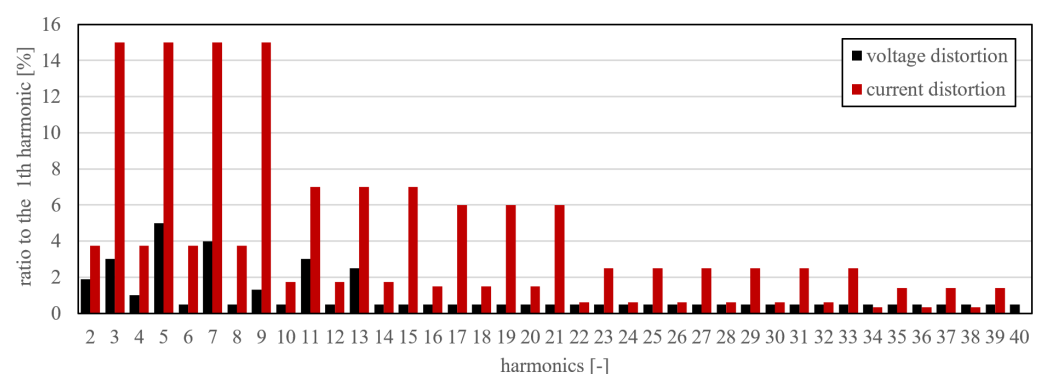


Figure 5. The levels of harmonic distortion relative to the fundamental frequency of 50 Hz.

4. Results

The calculation results for magnetic flux density are presented in Figure 6, and for electric field intensity are shown in Figure 7. From these results, we observe that the influence of harmonic content on the RMS value of electric field intensity is negligible, even when considering the maximum allowable voltage distortion defined by EN 50160:2022. Specifically, the maximum electric field intensity increased from 3.28 kV/m at the fundamental frequency to 3.30 kV/m when accounting for the entire spectrum, representing only a 0.4% increase. This minor increment becomes even less significant when factoring in the substantial impact of surrounding conductive and non-conductive objects—such as vegetation, structures, and fencing—on the electric field distribution around the OPL.

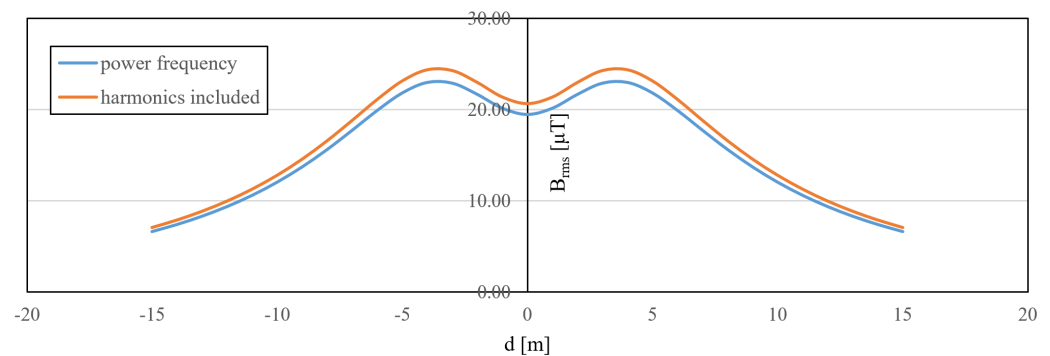


Figure 6. Results of magnetic flux density calculation for power frequency current, and with consideration of harmonics current distortion.

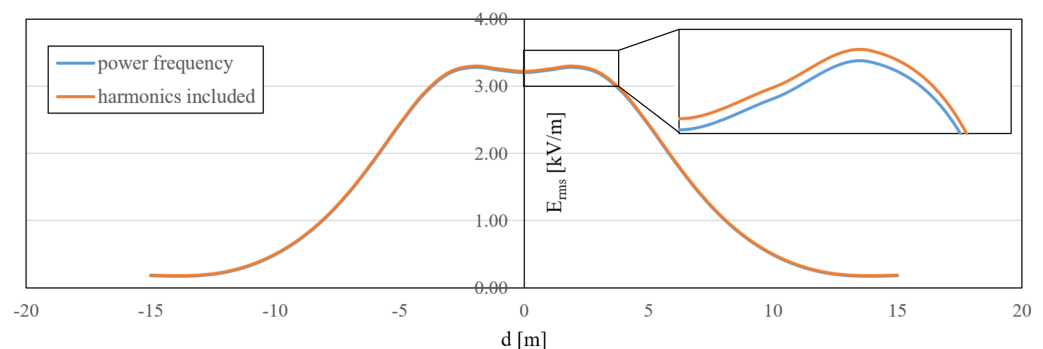


Figure 7. Results of intensity for the electric field calculation for power frequency voltage, and with consideration of harmonics voltage distortion.

Conversely, the magnetic flux density exhibits a more pronounced sensitivity to harmonic distortion in the current spectrum. The RMS value increased by 6.18%, from 22.97 μT at the fundamental frequency to 24.38 μT when including higher-order harmonics. This substantial rise is attributed to the presence of low-order harmonics, particularly the third and fifth, which are more prevalent in current waveforms due to non-linear loads and power electronic devices connected to the grid.

The occurrence and impact of these current harmonics vary across different voltage levels. Lower voltage levels are more susceptible to higher harmonic distortion because of the direct connection to numerous non-linear consumer loads, such as computers and LED lighting. However, these harmonics can propagate upstream to higher voltage levels through the network, especially if adequate filtering and mitigation measures are not in place. At medium and high voltage levels, industrial equipment and large-scale renewable energy sources equipped with power electronic interfaces can also introduce significant harmonic content into the system.

Due to the linearity of electromagnetic field interactions, a similar proportional increase can be expected in the induced voltages on buried pipelines located near OPL. Such increases pose a considerable risk to the proper functioning of cathodic protection systems, potentially

leading to accelerated corrosion and reduced structural integrity of the pipelines. Therefore, it is crucial to account for harmonic distortion effects in the design and analysis of OPLs and adjacent infrastructure to ensure operational safety and compliance with relevant standards.

5. Discussion

The following graph in Figure 8 shows the calculated percentage change in magnetic flux density as a function of current THD. Due to the linearity of the magnetic flux density and intensity in the air, the same chart applies to the electric field intensity. From the results, we observe that in the case of significant current THD levels (50%), the increase in the EMF components can be up to 10%. This finding can be applied to real measurements of current THD levels in 132 kV substations as cited in [36].

The results from [36] indicate that the maximum distortion in voltage ranges between 0.84% and 0.68%, with maximum values between 1.07% and 0.92%, and minimum levels between 0.40% and 0.52%. Even with an increase of up to 8%, as specified in EN 50160:2022, the influence remains insignificant. This influence would be even lower under EHV OPL where the harmonic levels in voltage are smaller [15]. However, the measurements in [36] showed that high levels of THD, up to 30% in current, are indeed possible and are often observed.

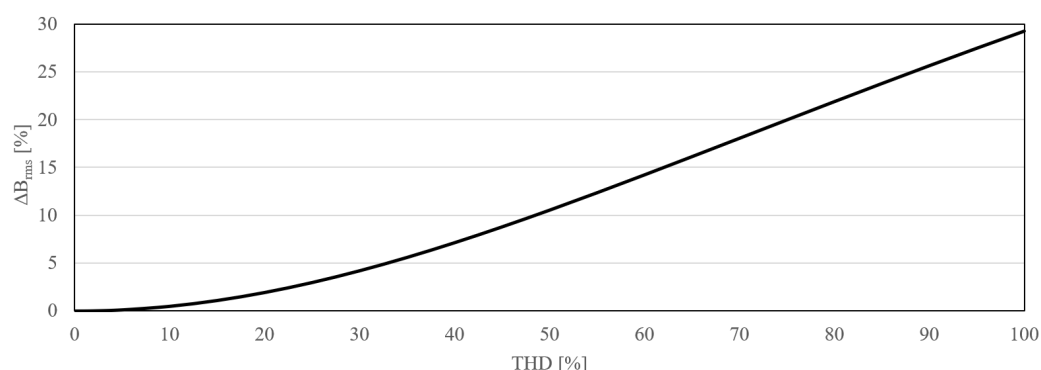


Figure 8. Change in the magnetic flux density RMS value as a function of current THD.

Figure 5 shows the significant difference between permissible harmonic content in voltages and currents. The logical results from this are that magnetic flux density will have a higher possibility of increasing above base frequency levels than the intensity of the electric field. This is also the result of our simulations.

A critical factor to consider is the potential increase in magnetic field induction. This magnetic field induction, characterized by inductive coupling, directly influences the induced voltages on buried steel pipelines. These voltages arise under steady-state conditions of the power line, particularly during worst-case scenarios like maximum line load. It is essential to limit these voltages to ensure the safe operation of the pipelines and minimize the risk of corrosion, which necessitates proper adjustments to their cathodic protection systems. Moreover, such calculations should be performed in a 3D context, as they are significantly more complex than presented here, allowing for a more accurate assessment of the interactions between the power line and the pipeline network.

6. Conclusions

This paper focuses on the calculation methods and results of extremely low-frequency electromagnetic fields, ELF around overhead power lines. Our study aimed to understand how these field levels are influenced by the presence of harmonic distortion in current and voltage waveforms. Detailed calculations were performed to assess the intensity of electric fields and magnetic flux density under scenarios involving Total Harmonic Distortion (THD) levels, in line with standards such as EN 50160:2022 and IEEE Std 519-2014.

The results indicate that harmonic distortion in current waveforms can significantly increase the RMS value of magnetic flux density by more than 5% when current harmonic distortion levels approach or exceed the established limits. In contrast, the effect of voltage harmonic

distortion on electric field intensity is minimal. This is because voltage harmonic distortion is typically lower and subject to stricter THD limits compared to current. The higher THD in the current often results from nonlinear industrial loads, which distort the current waveform. Additionally, system impedance at higher frequencies amplifies these harmonics, whereas voltage distortion is more effectively managed through filtering and damping techniques.

Implications for Safety:

- **Health Risks and ELF Exposure**—Understanding the influence of harmonic distortion on ELFF levels is crucial for assessing potential health risks. Our study highlights the need for careful monitoring and management of EMF exposure, particularly in areas where harmonic distortions are significant. While the increase in electric field intensity is minimal, the pronounced effect on magnetic flux density underscores the need for ongoing vigilance in managing EMF-related health concerns.
- **Infrastructure and Safety**—The study reveals that increased magnetic flux density due to harmonic distortion can affect surrounding infrastructure, such as buried pipelines. Elevated magnetic flux density can induce higher voltages in these pipelines, which may compromise the operation of cathodic protection systems and pose safety risks to personnel. Effective harmonic management and rigorous infrastructure monitoring are essential to prevent potential hazards and ensure the reliability of protective systems. Additionally, such calculations need to be conducted in 3D and are much more complex than presented here, allowing for a more accurate assessment of the interactions between the power line and the pipeline network.

In conclusion, while the electric field intensity remains largely unaffected by harmonic distortion, magnetic flux density emerges as a critical factor for measurement and validation. Future research will focus on the long-term measurements of magnetic flux density frequency spectra under high and extra-high voltage lines, comparing these results with simulation data to enhance our understanding and management of ELF in practical settings.

Author Contributions: Conceptualization, J.B. and M.C.; methodology, J.B.; validation, Ž.E. and M.C.; formal analysis, Ž.E.; investigation, J.B.; resources, M.C.; writing—original draft preparation, J.B.; writing—review and editing, M.C.; visualization, M.C.; supervision, Ž.E.; project administration, Ž.E. All authors have read and agreed to the published version of the manuscript.

Funding: This paper is supported by the agency VEGA MŠVVaŠ SR under Grant No.: VEGA 1/0390/23 and KEGA MŠVVaŠ SR under Grant No.: KEGA 026STU-4/2024.

Data Availability Statement: The original contributions presented in the study are included in the article, further inquiries can be directed to the corresponding author.

Conflicts of Interest: The authors declare no conflicts of interest.

Abbreviations

The following abbreviations are used in this manuscript:

OPL	overhead power line
EMF	electromagnetic field
ELF	extremely low frequency field
E	intensity of electric field
B	magnetic flux density
RMS	root mean square
WHO	World health organization
EHV	extra high voltage
HV	high voltage
ICNIRP	International Commission on Non-Ionizing Radiation Protection
AIMD	active implanted medical devices
THD	Total Harmonic Distortion
VSC	Voltage Source Converters
HVDC	High Voltage Direct Current

References

1. EPRI. *AC Transmission Line Reference Book—200 kV and Above*, 3rd ed.; Electric Power Research Institute: Washington, DC, USA, 2005.
2. International Telecommunication Union. *Nomenclature of the Frequency and Wavelength Bands Used in Telecommunications*; Electronic Publication: Geneva, Switzerland, 2015; p. 8.
3. Working Group 36.02. TB 95—*Guide on the Influence of high Voltage AC Power Systems on Metallic Pipelines*; CIGRE: Paris, France, 1995.
4. Rathebe, P.C.; Modisane, D.S.; Rampedi, M.B.; Biddesay-Manila, S.; Mbonane, T.P. A review on residential exposure to electromagnetic fields from overhead power lines: Electrification as a health burden in rural communities. In Proceedings of the 2019 Open Innovations (OI), Cape Town, South Africa, 2–4 October 2019; pp. 219–221. [\[CrossRef\]](#)
5. Frigura-Iliasa, M.; Baloi, F.I.; Frigura-Iliasa, F.M.; Simo, A.; Musuroi, S.; Andea, P. Health-Related Electromagnetic Field Assessment in the Proximity of High Voltage Power Equipment. *Appl. Sci.* **2020**, *10*, 260. [\[CrossRef\]](#)
6. Landini, M.; Mazzanti, G.; Mandrioli, R. Procedure for Verifying Population Exposure Limits to the Magnetic Field from Double-Circuit Overhead Power Lines. *Electricity* **2021**, *2*, 342–358. [\[CrossRef\]](#)
7. International Commission on Non-Ionizing Radiation Protection. Guidelines for Limiting Exposure to Time-Varying Electric and Magnetic Fields (1 Hz TO 100 kHz). *Health Phys.* **2010**, *99*, 818–836. [\[CrossRef\]](#) [\[PubMed\]](#)
8. Directive 2013/35/EU of the European Parliament and of the Council of 26 June 2013 on the Minimum Health and Safety Requirements Regarding the Exposure of Workers to the Risks Arising from Physical Agents (Electromagnetic Fields) (20th Individual Directive within the Meaning of Article 16(1) of Directive 89/391/EEC) and Repealing Directive 2004/40/EC, 2013. Available online: <https://eur-lex.europa.eu/legal-content/EN/TXT/?uri=celex%3A32013L0035> (accessed on 2 October 2024).
9. Directorate-General for Employment; Social Affairs and Inclusion (European Commission). *Non-Binding Guide to Good Practice for Implementing Directive 2013/35/EU Electromagnetic Fields—Guide for SMEs*; Publications Office: Luxembourg, 2015. [\[CrossRef\]](#)
10. Zhou, M.; Kourtiche, D.; Claudel, J.; Deschamps, F.; Magne, I.; Roth, P.; Schmitt, P.; Souques, M.; Nadi, M. Interference thresholds for active implantable cardiovascular devices in occupational low-frequency electric and magnetic fields: A numerical and in vitro study. *Med. Eng. Phys.* **2022**, *104*, 103799. [\[CrossRef\]](#) [\[PubMed\]](#)
11. Bendík, J.; Cenký, M.; Eleschová, Ž.; Belán, A.; Cintula, B.; Janiga, P. Comparison of electromagnetic fields emitted by typical overhead power line towers. *Electr. Eng.* **2020**, *103*, 1019–1030. [\[CrossRef\]](#)
12. Stam, R. *Comparison of International Policies on Electromagnetic Fields (Power Frequency and Radiofrequency Fields)* | ARPANSA; Technical Report; National Institute for Public Health and the Environment, RIVM: Bilthoven, The Netherlands, 2018.
13. VYHLÁŠKA Ministerstva zdravotníctva Slovenskej republiky o podrobnostiach o požiadavkách na zdroje elektromagnetického žiarenia a na limity expozície obyvateľov elektromagnetickému žiareniu v životnom prostredí. *Zb. Zak. č* **2007**, *534*, 3812–3816.
14. Turajlic, E.; Mujezinovic, A.; Alihodzic, A. A Comparative Analysis of Different Methods for Magnetic Induction Estimation in the Vicinity of Overhead Power Lines. In *2023 31st Telecommunications Forum (TELFOR)*; IEEE: Piscataway, NJ, USA, 2023. [\[CrossRef\]](#)
15. EN 50160:2022; Voltage Characteristics of Electricity Supplied by Public Electricity Networks. German Institute for Standardisation: Berlin, Germany, 2022.
16. IEEE Std 519-2014 (Revision of IEEE Std 519-1992); IEEE Recommended Practice and Requirements for Harmonic Control in Electric Power Systems. IEEE: Piscataway, NJ, USA, 2014; pp. 1–29. [\[CrossRef\]](#)
17. EN 50443:2011; Effects of Electromagnetic Interference on Pipelines Caused by High Voltage a.c. Electric Traction Systems and/or High Voltage a.c. Power Supply Systems. SUTN: Bratislava, Slovakia, 2011.
18. ISO 18086:2019; Corrosion of Metals and Alloys—Determination of AC Corrosion—Protection criteria. ISO: Geneva, Switzerland, 2019.
19. Lunca, E.; Ursache, S.; Salceanu, A. Computation and analysis of the extremely low frequency electric and magnetic fields generated by two designs of 400 kV overhead transmission lines. *Measurement* **2018**, *124*, 197–204. [\[CrossRef\]](#)
20. Jiang, Y.Z.; Liang, Z.G.; Ma, W.J.; Wang, H.C. Effect of Shielding Lines on Power Frequency Electric Field under Overhead Lines. *Adv. Mater. Res.* **2013**, *732–733*, 999–1004. [\[CrossRef\]](#)
21. Duane, I.; Afonso, M.; Paganotti, A.; Schroeder, M.A.O. Computation of the Electromagnetic Fields of Overhead Power Lines with Boundary Elements. In Proceedings of the 2022 IEEE 20th Biennial Conference on Electromagnetic Field Computation (CEFC), Denver, CO, USA, 24–26 October 2022; pp. 1–2. [\[CrossRef\]](#)
22. Lunca, E.; Ursache, S.; Salceanu, A. Characterization of the electric and magnetic field exposure from a 400 kV overhead power transmission line in Romania. In Proceedings of the 22nd IMEKO TC4 International Symposium and 20-th International Workshop on ADC Modelling and Testing, Iasi, Romania, 14–15 September 2017; pp. 239–244.
23. Elhabashi, S.M.; Ehtaiba, J.E. Electric fields intensity around the new 400kV power transmission lines in Libya. In Proceedings of the 6th WSEAS International Conference on Circuits, Systems, Electronics, Control& Signal Processing; Citeseer, Cairo, Egypt, 29–31 December 2007.
24. Machczyński, W.; Król, K. Optimization of electric and magnetic field intensities in proximity of power lines using genetic and particle swarm algorithms. *Arch. Electr. Eng.* **2018**, *67*, 829–843.
25. Olsen, R.G. Electromagnetic fields from power lines. In Proceedings of the 1993 International Symposium on Electromagnetic Compatibility, Dallas, TX, USA, 9–13 August 1993; IEEE: Piscataway, NJ, USA, 1993; pp. 138–143.

26. Lunca, E.; Vornicu, S.; Pavel, I.; Andrusca, M. Measurement and Numerical Simulation of the Low-Frequency Electric Field Generated by an Overhead Power Line. In Proceedings of the 2022 International Conference and Exposition on Electrical And Power Engineering (EPE), Iași, Romania, 20–22 October 2022; pp. 719–722, ISSN 2644-223X. [\[CrossRef\]](#)
27. Mujezinović, A.; Turajlić, E.; Alihodžić, A.; Dedović, M.M.; Dautbašić, N. Calculation of Magnetic Flux Density Harmonics in the Vicinity of Overhead Lines. *Electronics* **2022**, *11*, 512. [\[CrossRef\]](#)
28. Wu, T.; Xiao, B.; Liu, K.; Liu, T.; Peng, Y.; Su, Z.; Tang, P.; Lei, X. Study on Overhead Transmission Line Magnetic Field Harmonics of VSC-HVDC. In Proceedings of the 2016 IEEE International Conference ON High Voltage Engineering and Application (Ichve), New York, NY, USA, 19–22 September 2016.
29. Faria, J.A.B.; Almeida, M.E. Computation of transmission line magnetic field harmonics. *Eur. Trans. Electr. Power* **2007**, *17*, 512–525. [\[CrossRef\]](#)
30. Wu, J.; Guo, Q.; Yan, X.; Zhang, C. Theoretical Analysis on Affecting Factors of Power Line Harmonic Radiation. *IEEE Trans. Plasma Sci.* **2019**, *47*, 770–775. [\[CrossRef\]](#)
31. Mayer, D. *Aplikovaný Elektromagnetizmus : Úvod do Makroskopické Teorie Elektromagnetického Pole pro Elektrotechnické Inženýry*, 2nd ed.; Kopp: Baden, Germany, 2012.
32. Mayer, D.; Polák, J. *Metody řešení Elektrických a Magnetických polí*, 1st ed.; Nakladatelství Technické Literatury: Praha, Czech, 1983.
33. EPRI. *AC Transmission Line Reference Book—345 kV and Above*, 2nd ed.; Electric Power Research Institute: Washington, DC, USA, 1982; Chapter 7, pp. 329–417.
34. Bendík, J.; Kment, A.; Pípa, M. Enumeration of magnetic flux density generated by power transmission lines. In Proceedings of the 2015 16th International Scientific Conference on Electric Power Engineering (EPE), Kouty nad Desnou, Czech, 20–22 May 2015; pp. 396–401. [\[CrossRef\]](#)
35. Ippolito, M.G.; Puccio, A.; Ala, G.; Ganci, S.; Filippone, G. Mitigation of 50 Hz magnetic field produced by an overhead transmission line. In Proceedings of the 2015 50th International Universities Power Engineering Conference (UPEC), Stoke-on-Trent, UK, 1–4 September 2015; pp. 1–5. [\[CrossRef\]](#)
36. Albadi, M.H.; Al Abri, R.S.; Al Hinai, A.S.; Al-Badi, A.H. Harmonics Temporal Profile in High-Voltage Networks: Case Study. In *Power System Harmonics—Analysis, Effects and Mitigation Solutions for Power Quality Improvement*; IntechOpen: London, UK, 2017. [\[CrossRef\]](#)

Disclaimer/Publisher’s Note: The statements, opinions and data contained in all publications are solely those of the individual author(s) and contributor(s) and not of MDPI and/or the editor(s). MDPI and/or the editor(s) disclaim responsibility for any injury to people or property resulting from any ideas, methods, instructions or products referred to in the content.